Proceedings of the 8th U.S. National Conference on Earthquake Engineering
April 18-22, 2006, San Francisco, California, USA
Paper No. 1206

APPLICATION OF THE SPECIFIC BARRIER MODEL TO THE SIMULATION OF EARTHQUAKE STRONG GROUND MOTIONS

Benedikt Halldorsson[1] and Apostolos S. Papageorgiou[2]

ABSTRACT

The Specific Barrier Model provides a complete, yet parsimonious, self-consistent description of the heterogeneous earthquake faulting process. It assumes that the seismic moment is distributed in a deterministic manner on the fault plane, and is released through the incoherent rupture of identical "subevents" that fill the fault plane. Thus, the model can be applied in the "near-fault", as well as in the "far-field" region and has recently been calibrated using an extensive database of earthquake events representing three tectonic regimes (Halldorsson and Papageorgiou, 2005a). Using the parameters of the model that were obtained from the above calibration, we simulate time histories for a number of earthquake events that were well recorded, cover a wide magnitude range (M 5.9-7.9), and are representative samples of different source mechanisms. The stochastic approach is applied to synthesize the incoherent part of near- and far-field strong ground motion while the deterministic/coherent part of near-field strong motions is simulated using a recently proposed mathematical model of near-fault velocity pulses. We compare the simulations with the recorded data, both in the time and frequency domain and thus evaluate the overall performance of the model. It is shown that the model provides on the average unbiased predictions over a wide frequency range (0.1-20 Hz) of earthquake strong ground motions. Thus, the Specific Barrier Model can be utilized as an effective tool for providing time histories of near-fault and far-field earthquake ground motions that can be used with confidence by earthquake engineers in aseismic design.

Introduction

Relationships of strong ground motion attenuation are important for estimating the seismic hazard at a site. For regions where strong motion data is abundant, such as California, empirical relationships have been developed and successfully used in seismic hazard analyses. However, for regions where recorded ground motion data is scarce, such as Eastern North America, it becomes imperative to use physical models to represent the ground motion generation and propagation. Of the physical earthquake models available in the literature, the Specific Barrier Model (SBM) provides the most complete, yet parsimonious, self-consistent description of the earthquake faulting processes that are responsible for the generation of the high frequencies of ground motions, and at the same time provides a clear and unambiguous way of how to distribute the seismic moment on the fault plane. The latter requirement is necessary for synthesizing near-fault (i.e. in the vicinity of an extended source/fault) ground motions. Thus, the SBM applies both in the "near-fault" as well as in the "far-field" region, allowing for consistent ground motion simulations over the entire frequency range and for all distances of engineering interest. Furthermore, the model

[1]Research Engineer, Earthquake Engineering Research Centre, University of Iceland. Selfoss, IS-800, Iceland. Email: Benedikt.Halldorsson@gmail.com
[2]Professor. Department of Civil Engineering, University of Patras, Rio 26500, Greece. Email: papaga@upatras.gr

has been shown to capture effectively the essential characteristics of more complex seismic sources (Halldorsson, 2004; Halldorsson and Papageorgiou, 2005b). The SBM is particularly simple in application due to the few parameters needed, and because their scaling with magnitude has been established for different tectonic regions (Papageorgiou and Aki, 1983b; Papageorgiou, 1988; Aki and Papageorgiou, 1988; Aki, 1992; Beresnev and Atkinson, 2001; Halldorsson and Papageorgiou, 2005a)

In this study we use the SBM as calibrated by Halldorsson and Papageorgiou (2005a) to carry out "blind" strong motion simulations of several earthquakes, ranging in magnitude from $M_{\rm w}$ 5.9 - 7.9. By "blind" we mean that no other a-priori information on the earthquake source is required apart from the strike, dip, and the relative location of the hypocenter on the fault plane of a historical earthquake of a certain magnitude. The stochastic models obtained/calibrated by Halldorsson and Papageorgiou (2005a) are then used to simulate strong motion time histories. The stochastic assumption strictly is not valid below ~ 1 Hz. At near-fault stations however, we extend the validity of the simulations to lower frequencies by combining the high-frequency (incoherent) simulations with a low-frequency (coherent) near-fault time histories, using the mathematical model of Mavroeidis and Papageorgiou (2003). We compare the pseudo-spectral velocities of the data and synthetics and estimate the bias of the simulations to the data. We show that "blind" simulations of the SBM are on the average unbiased over a wide frequency range (0.1-20 Hz) of strong ground motions for other (i.e., not used in the calibration) earthquakes in a given tectonic regime. Furthermore, the addition of synthetic near-fault velocity pulses greatly improves the fit of the model to near-fault data. The self-consistency and parsimonious nature of the model therefore makes it an ideal tool for the simulation of strong ground motions for future events in a given tectonic setting. The SBM thus has important implications for earthquake engineering purposes, such as the fragility assessment of critical facilities (e.g., Wanitkorkul *et al.*, 2006), and aseismic structural design in general.

The Specific Barrier Model

The Specific Barrier Model was introduced and developed by Papageorgiou and Aki (1983a,b) for the quantitative description of heterogeneous rupture (see also Papageorgiou, 1988; Aki and Papageorgiou, 1988). According to the SBM the seismic fault may be visualized as an aggregate of circular subevents of equal diameter, $2\rho_\circ$ (the "barrier interval") filling up a rectangular fault of length L and width W, as shown schematically in Fig. 1. As the rupture front sweeps the fault plane with "sweeping velocity" V, a stress drop, $\Delta\sigma_L$, (referred to as the "local stress drop") takes place in each subevent starting from its center and spreading radially with constant "spreading velocity", ν.

The systematic magnitude-dependence of the main parameters of the SBM, the local stress drop, and the barrier interval inferred in the original studies by Aki and Papageorgiou has been confirmed by Halldorsson and Papageorgiou (2005a) for interplate earthquakes, and extended to intraplate earthquakes and earthquakes of regions of active tectonic extension. The local stress drop has been found to be a relatively stable parameter over a wide magnitude range: ~ 161 bar, 114 bar, and 180 bar for interplate, extensional, and intraplate earthquakes, respectively (Halldorsson and Papageorgiou, 2005a). Furthermore, the barrier interval increases with magnitude in a self-similar manner (see Fig. 2). This variation has furthermore been confirmed by Beresnev and Atkinson (2001), who use a model conceptually identical to the Specific Barrier Model.

The radiation of elastic waves emitted from each subevent as it breaks is based on a physical description of source processes using kinematic dislocation theory (Sato and Hirasawa, 1973).

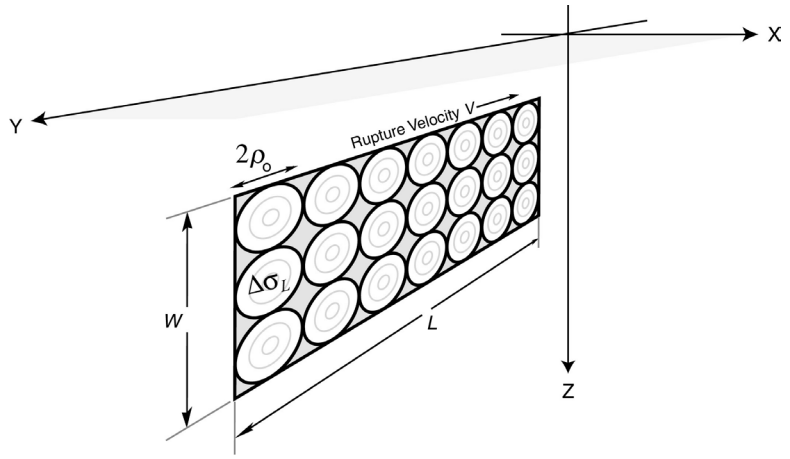

Figure 1. A schematic view of the specific barrier model of Papageorgiou and Aki (1983a,b). The fault plane consists of an aggregate of circular cracks with diameter $2\rho_\circ$ on a fault plane of length L and width W. A "local stress drop" $\Delta\sigma_L$ takes place in each crack as it ruptures. The rupture starts at the center of each crack and spreads radially outwards (the rupture fronts at successive time instants are denoted by the light circles) until it is arrested by the barriers, denoted by the shaded area between the cracks.

Papageorgiou and Aki (1983a) derived the far-field expression of the source spectrum radiated from such a crack, but for simplicity, the far-field source spectral shape of each subevent was approximated by an "ω-square" spectrum by Papageorgiou (1988) who also presented an expression for the far-field source spectrum for the *aggregate* subevent radiation (see also Joyner and Boore, 1986). Halldorsson and Papageorgiou (2005a) modified the expression by introducing a high-frequency source complexity factor, ζ into the expression for the far-field acceleration source spectrum of the SBM

$$S(M_\circ, f, \zeta) = \sqrt{N\zeta + N(N-\zeta)\left(\frac{\sin(\pi f T)}{\pi f T}\right)^2}\,(2\pi f)^2 \tilde{\dot{M}}_{o_i}(f) \tag{1}$$

where N is the number of subevents, T is the source duration, and $\tilde{\dot{M}}_{o_i}(f)$ is the source displacement spectrum of a single subevent. The high-frequency complexity factor accounts for the observed deviation of self-similar source scaling of earthquakes in interplate and extensional tectonic regimes (see Fig. 2a). To the first approximation, the factor varies with moment magnitude as follows

$$\log \zeta = 2 s_m \left(M_\mathrm{w} - M_c\right) \tag{2}$$

where $s_m - 0.12$ and $M_c = 6.35$. The physical origins of ζ presents an exciting research opportunity, and is under investigation in the context of the Specific Barrier Model (Halldorsson and Papageorgiou, 2005a).

The SBM distributes the seismic moment evenly over the fault plane, assuming identical subevents. Although this may appear to be too simplistic of an assumption for a complex earthquake source model, it is the natural one for "blind" strong motion modeling where the slip pattern of an earthquake has to be hypothesized. Moreover, if a higher degree of source complexity is required, it is simply implemented in the description of the subevents of the SBM. For example, the subevents may be allowed to vary in size (Halldorsson and Papageorgiou, 2005b), and/or be represented by a new family of sophisticated crack models (Dong and Papageorgiou, 2003).

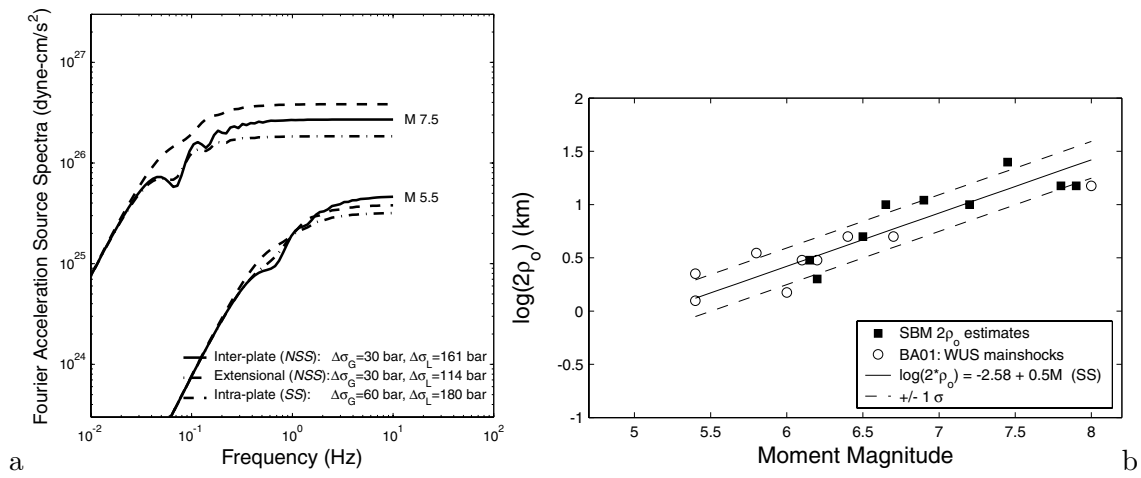

Figure 2. (a) The non-self-similar far-field S wave spectra of the specific barrier model for the inter-plate (solid), extensional (dot-dashed) and intra-plate (dashed) regime earthquakes, respectively. (b) Estimates of barrier interval (solid squares) vs. moment magnitude. The open circles are the subsource sizes of Beresnev and Atkinson (2001, BA01) for WUS mainshocks. The heavy solid line is the regression line to the estimates under the constraint of self-similarity. The dashed lines indicate the $\pm$ one standard deviation of the regression line.

We apply the SBM in the context of the stochastic modeling approach (stochastic method) in synthesizing strong ground motions time histories. For details on the model and relevant parameters the reader is referred to Halldorsson and Papageorgiou (2005a). In the far-field region the high-frequency radiation from the subevents of the SBM sums up incoherently (e.g., Papageorgiou and Aki, 1983a) and their aggregate spectrum is described by Eq. (1). The far-field assumption however, is not valid at near-fault sites. For each site in the near-fault region therefore, we synthesize time histories from each *subevent* separately. The synthetic motions from the N subevents are then summed up at the site, appropriately lagged in time. As we use available information on the relative hypocentral location on the fault plane, synthesizing the strong motion in this manner results in more realistic time histories because directivity effects are to a large extent taken into account.

Although the SBM was calibrated using spectral response data in the frequency range of $0.5-10.0$ Hz we allow the comparison with data at frequencies $0.1-20.0$ Hz. Below approximately 1.0 Hz the stochastic assumption is, strictly speaking, not valid due to coherent wave components dominating the motions. Furthermore, in the near-fault region of an earthquake fault, depending on magnitude, there can be a prominent coherent signal in the form of near-fault velocity pulses, characterized by their large amplitude and period. Mavroeidis and Papageorgiou (2003) presented a mathematical expression for near-fault velocity ground motions (their Eq. 3)

$$v(t) = \begin{cases} A\frac{1}{2}\left[1+\cos\left(\frac{2\pi f_P}{\gamma}(t-t_0)\right)\right]\cos\left[2\pi f_P(t-t_0)+\nu\right] & ; t_0-\frac{\gamma}{2f_P} \le t \le t_0+\frac{\gamma}{2f_P} \\ 0 & ; \text{otherwise} \end{cases} \quad (3)$$

In their phenomenological model the parameter A controls the amplitude of the signal, f_P is its prevailing frequency, ν is the phase of the amplitude-modulated harmonic, γ is a parameter that defines the oscillatory character (i.e., zero-crossings) of the signal, and t_0 specifies the epoch of

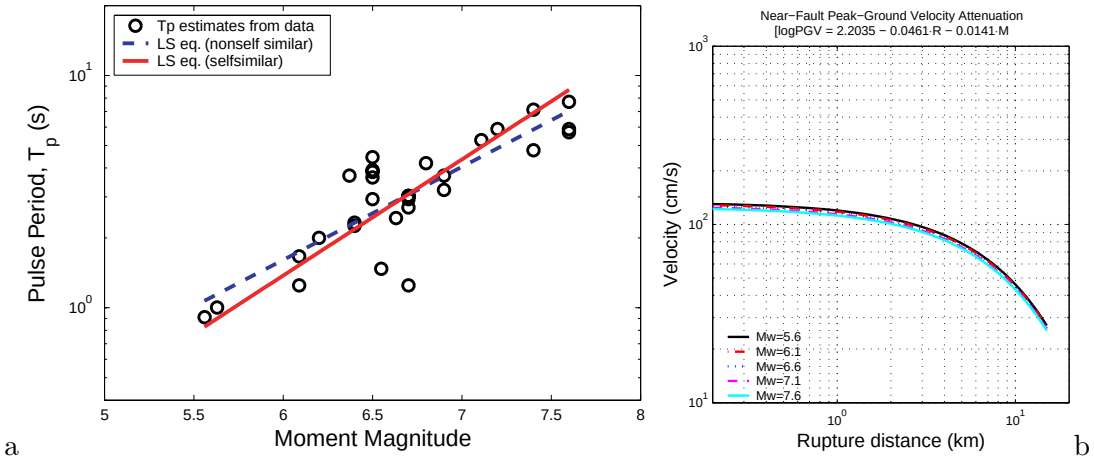

Figure 3. (a) Scaling of the pulse period with magnitude (Mavroeidis and Papageorgiou, 2003). (b) Peak ground velocity [PGV, $A \sim (0.85 - 1.00)$PGV] attenuation with distance and magnitude.

the envelope's peak. The near-fault motions that they analyzed were characterized by velocity pulses (along the fault-normal direction) in the time domain with a dominant period that scales self-similarly with earthquake magnitude: ranging from a few to almost ten seconds with increasing magnitude. The dependence of the prevailing period ($T_P = 1/f_P$) with magnitude is shown in Fig. 3a and is

$$\log T_P = -2.9 + 0.5M_{\rm w} \tag{4}$$

Furthermore, the amplitudes of the pulses from stations within 7 km were found to have a near-constant value of around $A = 73$ cm/s ($A \sim [0.85 - 1.00]$PGV) and in general, the model amplitude dependence with magnitude and distance can effectively be captured by the empirical relation

$$\log PGV = 2.204 - 0.046R_{rup} - 0.014M_{\rm w} \tag{5}$$

and is plotted in Fig. 3b. Note especially the very slight dependence of the amplitude with magnitude. [Parenthetically we note the apparent lack of correlation of these parameters with site conditions and slip types (Mavroeidis *et al.*, 2005).]

We obtained the means and standard deviations of the parameters of the mathematical model in Eq. (3) from the fitting to near-fault data by Mavroeidis and Papageorgiou (2003). For each $M_{\rm w}$-R_{rup} (event-station) pair within 20 km from the fault we generate a near-fault time history, allowing for certain randomness of the parameters as stipulated by the set of near-fault pulse parameters inferred from data. For stations in the near-fault region we combined the near-fault time histories with the high-frequency synthetics from the SBM according to the procedure described in Mavroeidis and Papageorgiou (2003), aligning the onset of the near-fault pulse that of the earliest signal from the subevents at the station. Assuming lognormal distribution of A and f_P and normal distributions of γ, ν we generated a set of random near-fault time-histories for each near-fault station. This above procedure is schematically shown in Fig. 4a-d, resulting in hybrid strong motion time histories for comparison with the recorded data in our dataset. This is applied only to the strike-normal component. There does at present not exist enough data for a robust regression on pulse parameters associated with the fault-parallel component, which additionally appears to be controlled by other source parameters than the fault-normal component (Mavroeidis *et al.*, 2005).

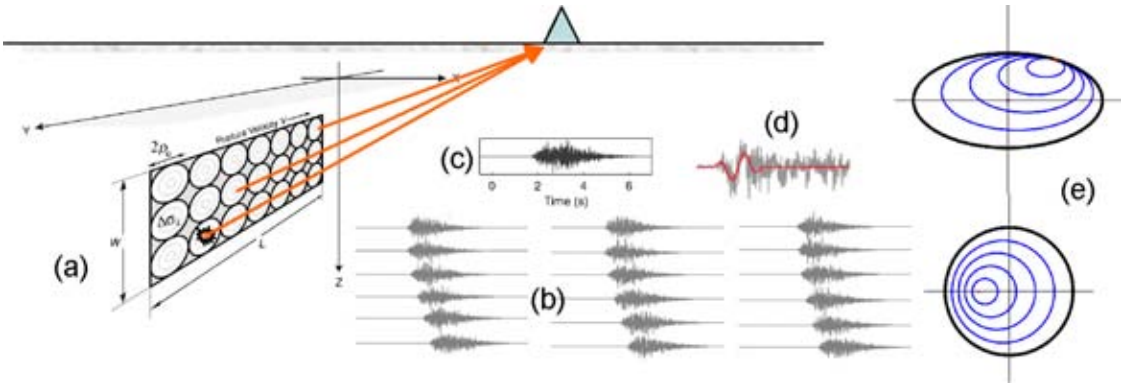

Figure 4. (a) Schematic view of the specific barrier model for a hypothetical earthquake source and near-fault station. (b) Individual subevent time history simulations at the site, appropriately lagged in time. (c) The sum of the subevent time histories at the site. (d) Schematic view of the superposition of incoherent (short-period), and coherent (long period near-field pulse) parts of strong ground motion. (e) Simplified view of two members of a new family of subevent (crack) models that can be implemented in the specific barrier model in a straighforward way (Halldorsson, 2004). The blue thin lines indicate the subevent rupture front at successive time instants.

Data

We selected a number of well recorded earthquakes, listed in Table 1, covering a relatively wide magnitude range from $M_{\rm w}$ 5.9 to 7.9 and have collected the data (corrected acceleration, velocity and displacement time histories) from online data repositories (e.g., COSMOS and ISESD[3]). We obtained finite-source rupture models for each of the events from various sources, most of them from the Online Database of Finite-Source Rupture Models[4]. The data recorded in the near-fault region was baseline corrected and the horizontal components rotated parallel and perpendicular to the strike of the earthquake. The recording sites were grouped according to their assigned NEHRP classes with A-C classified as rock and CD-D as soil, respectively (see Halldorsson and Papageorgiou, 2005a, for more information).

Results

Due to space limitations we show results only pertaining to the Chi-Chi earthquake (for other events, see Halldorsson *et al.*, 2004). We applied the SBM model and synthesized a subset of the strong motion data recorded during the 1999 Chi-Chi earthquake. We included all the strong motion stations that were closest to the surface rupture of the earthquake, and randomly selected approximately 100 stations that were farther from the fault. Fig. 5 shows the surface expression of the fault rupture, the vertical projection of the SBM for this earthquake, the epicentral location, and the strong motion stations used. As an example of the strong motion simulation procedure for near-fault stations we show the recorded and synthetic fault-normal strong motion time histories for station TCU075 (see also Fig. 6 for station TCU128). Shown are the recorded acceleration, velocity and displacement (top left), the corresponding high-frequency (black) and the low-frequency (gray) synthetic near-fault motions (top right), the combined broad-band synthetic of the high- and low-frequency motions (middle right), and the corresponding PSV comparison of the data and the

[3]COSMOS: `http://www.seismo.ethz.ch/srcmod/`. ISESD: `http://www.isesd.hi.is/`.
[4]Compiled by Dr. Martin Mai, see `http://www.seismo.ethz.ch/srcmod/`.

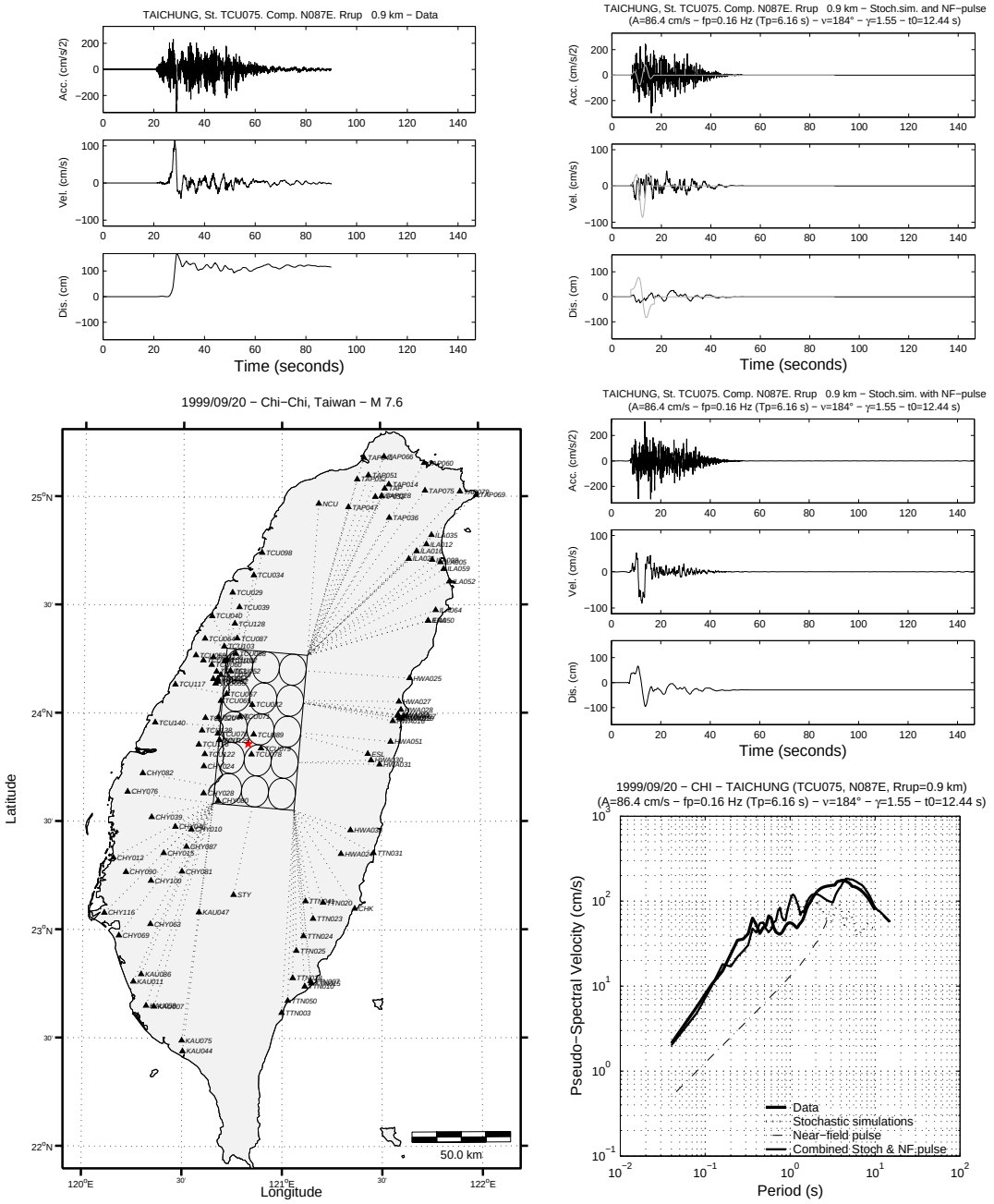

Figure 5. Bottom left: Map of Taiwan showing the vertical fault plane projection of the SBM for the Chi-Chi earthquake and the stations used in the analysis. The thick solid line denotes the mapped surface expression of the fault. Top left: The recorded strike-normal acceleration, velocity and displacement strong motion at station TCU075. Top right: The corresponding incoherent (black) and a coherent (near-fault pulse, gray) synthetics. The plot below shows the combination of the two, resulting in broad-band near-fault synthetics. Bottom right: The corresponding PSV comparisons of data (thick solid line) and broad-band synthetics (thin solid line). The synthetics are made up of the incoherent (dotted) and the coherent (near-fault pulse, dot-dashed) parts of ground motions.

Table 1. List of earthquake events used in this study. The number of stations used for each earthquake is denoted by n.

No.	Date	Event name	Region	Lat. (°N)	Lon. (°E)	$M_{\rm w}$	Dep. (km)	Strike (°)	Dip (°)	n
1	1986/07/08	North Palm Springs	S. CA, USA	33.999	-116.608	6.2	11.1	300	45	31
2	1987/11/24	Superstition Hills	CA, USA	33.013	-115.838	6.6	2.0	125	80	7
3	1994/01/17	Northridge	S. CA, USA	34.209	-118.540	6.7	19.0	122	44	144
4	1999/08/17	Izmit-Kocaeli	Turkey	40.639	29.830	7.4	17.0	91	87	21
5	1999/09/07	Athens	Greece	38.110	23.570	5.9	8.0	115	57	17
6	1999/09/20	Chi-Chi	Taiwan	23.860	120.800	7.6	10.3	357	29	120
7	2000/06/17	South Iceland	Iceland	63.970	-20.360	6.5	6.3	4	86	14
8	2000/06/21	South Iceland	Iceland	63.970	-20.710	6.5	5.1	2	85	13
9	2002/11/03	Denali	AK, USA	63.517	-147.525	7.9	5.0	294	86	6

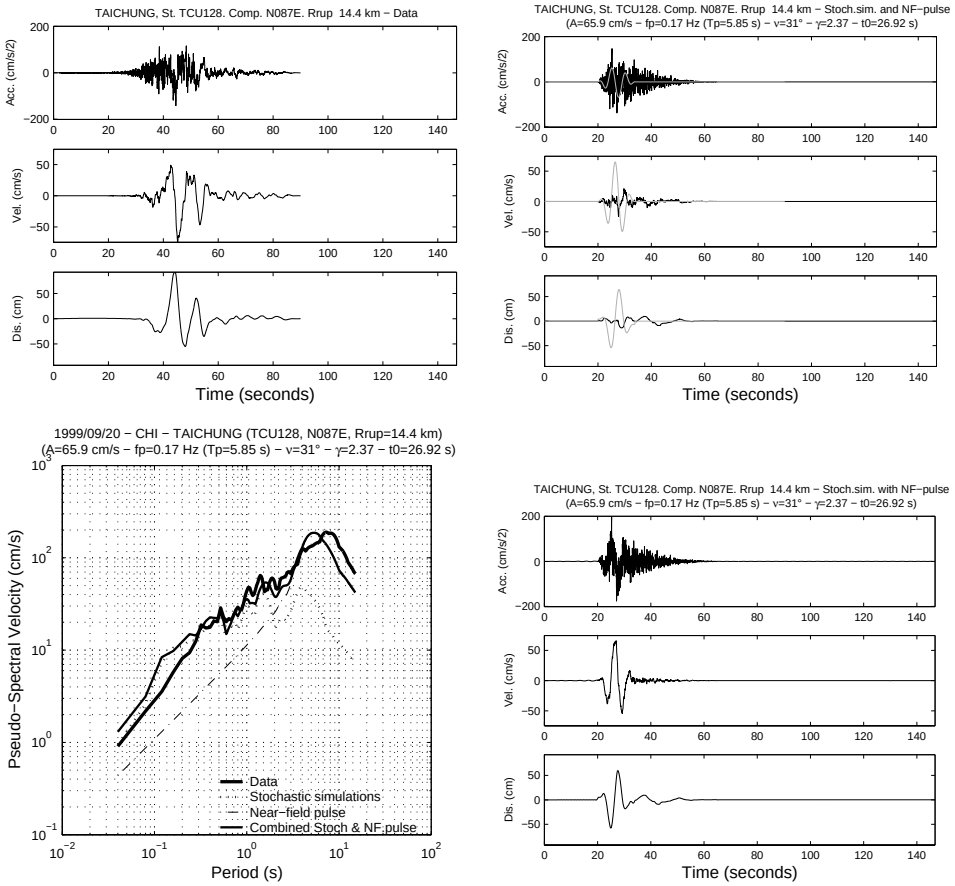

Figure 6. Same as in Fig. 5 except for station TCU128.

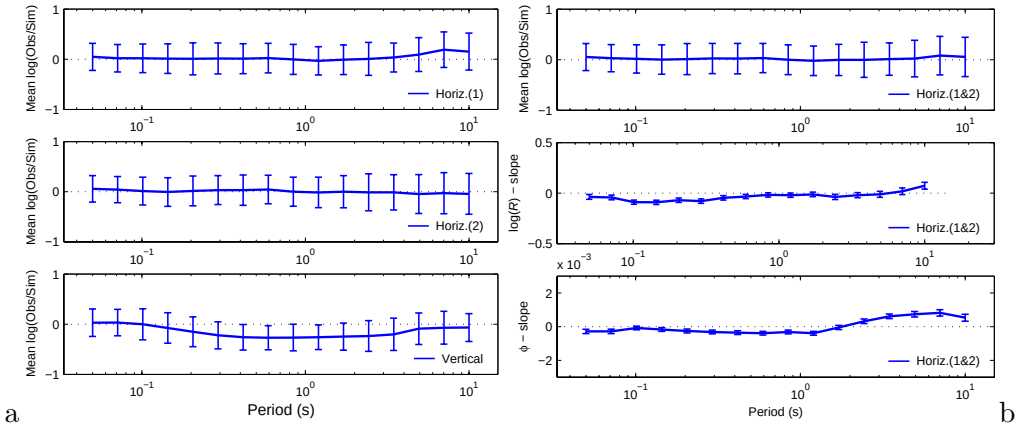

Figure 7. (a) The mean residual bias (log(data/sim.)) and the +/- one standard deviations for the first (top), and second (middle) horizontal, and the vertical (bottom) components of motion, plotted vs. oscillator period from 0.05-10 seconds (0.1-20 Hz). (b) The mean residual bias of the geometric mean of the two horizontal components in (a) (top), and the slopes of a straight line fitted through the residuals plotted vs. log-distance (middle) and azimuth (bottom).

synthetics (bottom right). The thick solid line is the PSV of data, the thin dot-dashed line is the PSV of the near-fault pulse, the dotted line is the PSV of the stochastic simulations and the thin solid line is the combination of the stochastic simulations and the near-fault pulse. Comparing the dotted line vs. the thin solid line at periods larger than 1 second clearly shows how the inclusion of the random near-fault pulse improves the fit.

A concise presentation of the overall fit of the SBM to six interplate events in Table 1 (nos. 1,3,4,6,7,8) is shown in Fig. 7a in which the mean residual bias (log(data/sim.)) and the $\pm$ one residual standard deviations for the first (top), and second (middle) horizontal, and the vertical (bottom) components of motion, are plotted vs. oscillator period from 0.05-10 seconds (0.1-20 Hz). Fig. 7b shows the mean residual bias of the geometric mean of the two horizontal components in (a) (top), and the slopes of a straight line fitted through the residuals plotted vs. log-distance (middle) and azimuth (bottom). As can be seen the modeling results in essentially zero bias over the entire range of oscillator frequencies for the above interplate events. The modeling did not include the vertical component, hence the overprediction of the model vs. the data (see Halldorsson *et al.*, 2005). The synthetic motions underpredict the first horizontal component (fault-parallel) at large periods because near-fault motions were not synthesized for this case. Note however the complete lack of large period bias for the second horizontal component, which is the fault-normal component to which the near-fault synthetics were added.

Conclusions

The SBM as calibrated by Halldorsson and Papageorgiou (2005a) has been shown to provide on the average unbiased predictions over a wide frequency range (0.1-20 Hz) of strong ground motions for other (i.e., not used in the calibration) earthquakes in a given tectonic regime. Furthermore, the addition of synthetic near-fault velocity pulses using the mathematical model of Mavroeidis and Papageorgiou (2003) greatly improves the fit of the model to near-fault data. The self-consistency and parsimonious nature of the model therefore makes it an ideal tool for fast and efficient simulation of strong ground motions for future events (i.e., "blind" simulations) for a given

tectonic setting. This in turn has important implications for earthquake engineers concerned with increasing the reliability of site-specific design of earthquake resistant structures.

Acknowledgements

This work was supported by Contract Numbers MCEER 00-0102, 01-0102, 02-0102, 03/0.1, and 04-0001 under the auspices of the Multidisciplinary Center for Earthquake Engineering Research (MCEER), and by the National Science Foundation, Award Number EEC-9701471. The first author would like to thank Prof. Andre Filiatrault at the University at Buffalo for his support.

References

Aki, K. (1992). Higher-order interrelations between seismogenic structures and earthquake processes, *Tectonophysics* 211, 1–12.

Aki, K. and A. S. Papageorgiou (1988). Separation of source and site effects in acceleration power spectra of major California earthquakes, in *Ninth World Conference on Earthquake Engineering*, volume Vol. VIII, SB-8, Tokyo-Kyoto, Japan.

Beresnev, I. and G. M. Atkinson (2001). Subevent structure of large earthquakes - A ground-motion perspective, *Geophys. Res. Lett.* 28, 53–56.

Dong, G. and A. S. Papageorgiou (2003). On a new class of kinematic models: Symmetrical and asymmetrical circular and elliptical cracks, *Phys. Earth. and Planet. Int.* 137, 129–151, doi: 10.1016/S0031-9201(03)00012-8.

Halldorsson, B. (2004). *The Specific Barrier Model: Its Calibration to Earthquakes of Different Tectonic Regions and the Synthesis of Strong Ground Motions for Earthquake Engineering Applications*, Ph.D. thesis, University at Buffalo, State University of New York, Buffalo, New York.

Halldorsson, B., G. Mavroeidis, F. Zhang, G. Dong, and A. S. Papageorgiou (2004). Simulation of strong ground motion using the specific barrier model, American Geophysical Union, Fall Meeting, San Francisco, California, December 13.-16.

Halldorsson, B., S. Olafsson, and R. Sigbjornsson (2005). Simulation of far-field and near-fault strong motions of the June 17 and 21, 2000, earthquakes in South Iceland, *Bull. Earthq. Eng.* (In review.).

Halldorsson, B. and A. S. Papageorgiou (2005a). Calibration of the specific barrier model to earthquakes of different tectonic regions, *Bull. Seism. Soc. Am.* 95, 1276–1300, doi: 10.1785/0120040157.

Halldorsson, B. and A. S. Papageorgiou (2005b). Sensitivity of far-field spectra of a composite seismic source model to different subevent size distributions and rupture times, (Manuscript in preparation.).

Joyner, W. B. and D. M. Boore (1986). On simulating large earthquakes by Green's function addition of smaller earthquakes, in S. Das et al. (Editor) *Earthquake Source Mechanics, Maurice Ewing Series*, volume 6, Am. Geophys. Union.

Mavroeidis, G. P., B. Halldorsson, and A. S. Papageorgiou (2005). Modeling and simulation of near-fault strong ground motions for earthquake engineering applications. (Manuscript in preparation.).

Mavroeidis, G. P. and A. S. Papageorgiou (2003). A mathematical representation of near-field ground motions, *Bull. Seism. Soc. Am.* 93, 1099–1131.

Papageorgiou, A. S. (1988). On two characteristic frequencies of acceleration spectra: Patch corner frequency and $f_{\max}$, *Bull. Seism. Soc. Am.* 78, 509–529.

Papageorgiou, A. S. and K. Aki (1983a). A specific barrier model for the quantitative description of inhomogeneous faulting and the prediction of strong ground motion. I. Description of the model, *Bull. Seism. Soc. Am.* 73, 693–722.

Papageorgiou, A. S. and K. Aki (1983b). A specific barrier model for the quantitative description of inhomogeneous faulting and the prediction of strong ground motion. Part II. Applications of the model, *Bull. Seism. Soc. Am.* 73, 953–978.

Sato, T. and T. Hirasawa (1973). Body wave spectra from propagating shear cracks, *J. Phys. Earth* 21, 415–431.

Wanitkorkul, A., B. Halldorsson, A. S. Papageorgiou, and A. Filiatrault (2006). Application of the specific barrier model to the seismic fragility assessment of critical facilities, in *8th U.S. National Conference on Earthquake Engineering (8NCEE)*, EERI, San Francisco, California, 18.–22. April 2006.